Water-Rock Interaction in Tarim Basin: Constraints from Oilfield Water Geochemistry *

CAI CHUNFANG (蔡春芳), MEI BOWEN (梅博文)

(Organic Geochemistry Lab., Jianghan Petroleum Institute, Jingzhou, 434102)

LI WEI (李 伟)

(Petroleum Exploration and Development Institute, Beijing, 100083)

AND ZENG FANGANG (曾凡刚)

(Geology Department of Peking University, Beijing, 100871)

Abstract: Oilfield waters from Cenozoic and Mesozoic terrestrial and Paleozoic marine environments in the Tarim Basin show no obvious difference in water chemistry except Br and isotopic compositions. The Paleozoic marine strata have higher Br concentrations than the terrestrial sediments, and the lack of obvious relationship between Br and I suggests that Br is not, for the most part, derived from the degradation of organic matter. The oilfield waters are characterized by high TDS (total dissolved solids), ranging from 120000 mg/L to 320000 mg/L, relatively low Mg, high Ca, Sr, and CF relative to Br of evaporating seawater, suggestive of enhanced water-rock interaction. OAA (organic acid anions) concentrations are generally lower than 1500 mg/L with high values occurring over the temperature range from 95°C to 140 °C, in the Cambrian to Jurassic systems, and nearby unconformities. Organic acids are considered to be generated mainly from thermal maturation of kerogens during progressive burial of the Jurassic-Triassic and Cambrian-Ordovician systems, biodegradation of crude oils nearby unconformities, and thermochemical sulfate reduction in part of the Cambrian and Ordovician strata. High Al concentrations up to 3 mg/L to 5.5 mg/L tend to occur in the waters of high OAA or petroleum-bearing intervals, suggesting the presence of organic complexing agents. Calculation by SOLMINEQ. 88 with updated database shows that $AlAc^{2+}$ may account for more than 30% of the total Al. Isotopic measurements (δD, $\delta^{18}O$) provide evidence for the following types of waters: diagenetically-modified connate meteoric water from the Jurassic and Triassic strata; diagenetically-modified connate marine water from the Cambrian and Ordovician strata; sub-aerially-evaporated water from the Cenozoic and Cretaceous strata; and mixed meteoric-evaporated or/and diagenetically modified connate water from the Carboniferous strata and reservoirs adjacent to the J/C and T/C unconformities. Those waters with very negative δD values from $-51.30‰$ to $-53.80‰$ (SMOW) and positive $\delta^{18}O$ values from 2.99‰ to 4.99‰ (SMOW) in the continuous burial of the Cambrian-Ordovician system are explained to have resulted from hydrocarbon-water and water-rock interactions.

Key words: water-rock interaction; oilfield water geochemistry; hydrogen and oxygen isotopes; Tarim Basin

Introduction

The origin and chemical evolution of oilfield waters in sedimentary basins are a perplexing problem. A simple connate origin was adovated early (White, 1965), and complete flushing by meteoric waters was suggested to explain hydrogen and oxygen isotope distribution (Clayton et al., 1966; Kharaka et al., 1985). Recently, evapo-concentrated seawater, which was diluted by infiltration of meteoric water (Knauth and Beeunas, 1986; Connolly and Walter, 1990b;

Egeberg and Aaggaard, 1989; Wilson and Long, 1993a), and wholly subaerially evaporated seawater (Wilson and Long, 1993b) were proposed. Additionally, diagenetically-modified connate water type (Land and Macpherson, 1992; Fisher and Boles, 1990), and the mixture of diagenetically-modified connate water and meteoric water (Fisher and Boles, 1990) were also identified. In China, most research work has focused on the hydrogeology and isotope geochemistry of subsurface waters. Whereas in the Tarim Basin, only hydrogeological characteristics have been reported, but the origin and evolution of oilfield waters remain unknown. This paper presents the analytical results of major elements for 419 oilfield waters from different wells or different intervals of the same well, 63 Br and I, and 73 hydrogen and oxygen isotopes, 185 organic acid anions, with an attempt to expound the origin and evolution of oilfield waters from the Tarim Basin, especially the effect of water-rock interaction.

Geological Setting and Analytical Method

The Tarim Basin borders on the Tianshan Mountains in the north, the Kunlun Mountains in the southwest, and the Aerjin Mountains in the southeast, has a total area of 560000 km^2, which is the largest oil-bearing sedimentary basin in China. It may be subdivided into 3 uplifts, including North Tarim, Central Tarim and South Tarim, and 4 depressions, including Keche, Northern, Southwestern, and Southeastern Tarim, in which the North and Central Tarim Uplifts are the main oil and gas reservoir areas. There exist 6 major unconformities essentially extending to the whole basin, below or above which lie AnZ, Zx and $\in$-O, S, D, C, K-J-E and/ or T, N and Q strata. The Cambrian and Ordovician strata are composed mainly of grey and dark grey dolomite, limestone and mudstone, which are considered to be the main oil source rocks. The Silurian and Upper Paleozoic rocks are marine clastic sediments, the Mesozoic and Cenozoic strata are composed mainly of terrestrial sandstone and mudstone, but seawater incursion is suspected to occur during the Triassic and Jurassic periods in the Kuche depression.

The waters described in the paper are produced from the Cambrian-Ordovician, Carboniferious, Mesozoic and Tertiary strata from the North and Central Tarim Uplifts. The samples were obtained through drillstem testing and separators on producing wells. Hydrogen and oxygen isotopes were analyzed at the State Open Laboratory of Isotope Analysis in Yichang, Hubei. Organic acid anions were analyzed by means of isotechophoresis at the Organic Geochemistry Laboratary of Jianghan Petroleum Institute, and the results are in accord with those analyzed by Barth (pers. com., 1991). Minor and trace metallic elements were analyzed by inductively coupled plasma at the Environment and Ecology Institute of China.

Results and Discussion

Oilfield waters are characteristic of high total dissolved solids (TDS), in the range of 40000 mg/L to 320000 mg/L, mainly 120000 mg/L to 220000 mg/L with an average value of 152118 mg/L, the highest among all oil-bearing basins in China. According to the water classification of Hem (1970), all the waters are brines (TDS > 35000 mg/L). Scatter diagram (Fig. 1) shows no obvious correlation between TDS and depth, which contrasts with universal idea, and that TDS are related to: (i) lithology, and (ii) mixing near the unconformities. In general, waters with high TDS from 220000 mg/L to 320000 mg/L occur in Tertiary and partial Carboniferious strata containing halite minerals, even halite bedding or salt diapire. And waters in carbonate reservoirs are characterized by relatively low TDS, ranging from 120000

mg/L to 140000 mg/L. Another characteristic is that waters with low TDS from 40 mg/L to 80000 mg/L are found in the Ordovician, Silurian and Carboniferous strata beneath regional unconformities. For example, waters near the J/C unconformity in the Well DH2 section have lower TDS from 20000 mg/L to 30000 mg/L than those far away from the uncomformitity, and are relatively enriched in Na and HCO_3. A positive correlation occurs between chloride concentrations and TDS, and chloride generally accounts for 60% ± 2% of TDS (Table 1). Ternary diagram of major cations K + Na, Ca, Mg (Fig. 2) shows that K + Na abundance ranging from 75 mole% to 95 mole%, Ca from 5 mole% to 25 mole%, Mg from 1 mole% to 2 mole% of the total K + Na, Ca, Mg in general, and they may be identified as partially Mg-depleted waters according to the classification by Fisher and Boles (1990). This composition pattern characterized by relative depletion of Mg and abundance of Ca is explained for the dolomitization of calcite and plagioclase dissolution. It is impossible that Ca is mainly supplied by the dissolution of calcite because the concentrations of Ca are 20 times higher than those of HCO_3(Table 1).

$$2CaCO_3 + Mg^{2+} = CaMg(CO_3)_2 + Ca^{2+}$$
$$CaAl_2Si_2O_8 + H^+ = Al_2Si_2O_5(OH)_4 + Ca^{2+}$$

According to calculations by Land and Macpherson (1992), the dissolution of 30 cm^3 anorthite in 1L of water can produce 15000 mg Ca^{2+}/L, which may occur in Triassic and Carboniferous sandstones of about 19% – 22% porosity, and Ca concentrations are generally less than 13000 mg/L (Table 1), so it is possible for Ca to be released by plagioclase dissolution in the above formations. All Cl abundance is higher than 96 mole%, and SO_4 less than 3 mole% of the total of Cl + SO_4 HCO_3. Low SO_4 concentrations result from bacterial sulfate reduction, i. e., BSR (Cai et al., 1996a) or thermochemical sulfate reduction (TSR) (Cai et al., 1997).

Minor and trace elements

Aluminum   Aluminum is one of the major elements contained in alumino-silicate minerals such as feldspar, muscovite, quartz and clay, so their distributions are expected to provide information on water-rock interactions. Analysis of 123 oilfield water samples shows that aluminum ranges from 0.36 mg/L to 5.40 mg/L, mostly from 1 mg/L to 3 mg/L (Fig. 3), much greater than < 20μg/L Al concentrations (Kharaka et
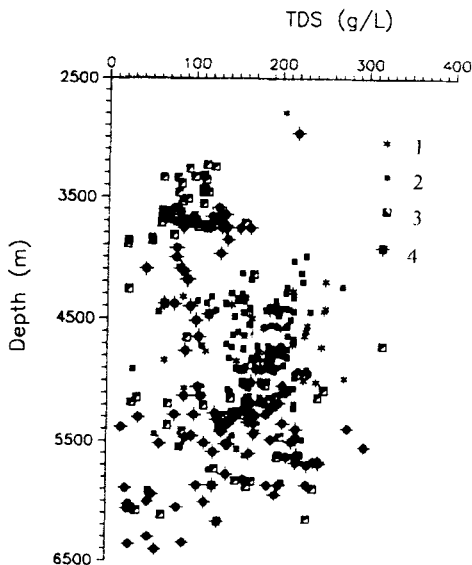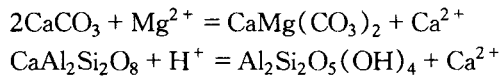

Fig. 1. Scatter diagram showing no covariation between TDS and depth for all water samples, suggesting that TDS are related to lithology and mixing. 1. Cenozoic; 2. Mesozoic; 3. Upper Palaeozoic; 4. Lower Palaeozoic

al., 1986). And it can be seen that there exists up to 5.35mg/L Al and 2571.44 × 10^{-6} OAA in the depth interval of 5981.59 – 6160 m in the Ordivocian strata in Well LN13, and 5.40 mg/L and 4.43 mg/L Al can also be found in oil-bearing strata at the depth of 4093 – 4181 m in Well TZ2 and of 5940 – 5953 m in Well YM2, respectively. Relatively high Al concentrations are
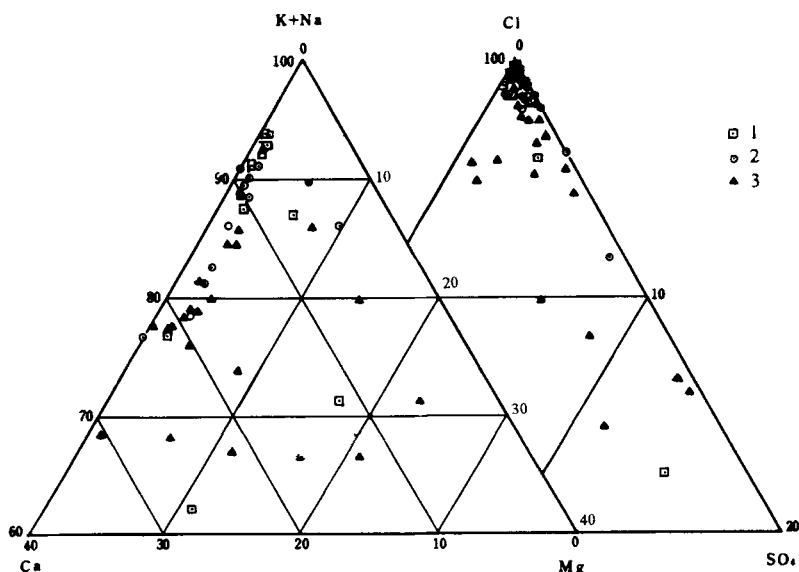
Fig. 2. Triangular diagrams of major cations K + Na, Ca, Mg and anions Cl, SO₄, HCO₃, showing relative mole percentages. 1. Carboniferous and Silurian; 2. Mesozoic and Cenozoic; 3. Lower Palaeozoic

Table 1. Average chemical compositions of oilfield waters from different systems

Age	N	E	K	J	T	C(LN)	C(DH)	C(TZ)	∈-O
No.	15-2-5	11-5-1	17-9-9	43-18-6	88-26-24	34-9-2	15-6-2	58-29-20	113-19-5
TDS	202937	193281	178867	169549	170099	145980	174861	83747	140568
Cl	121251	117346	108126	104097	103640	90224	105114	59226	83684
SO₄	2573	1479	1873	2640	1956	2189	1533	1516	2119
HCO₃	197	124	187	142	142	216	322	330	351
K + Na	73991	62530	56583	56764	59478	41895	60232	25877	40180
Mg	400	1055	861	1098	861	1513	466	512	1430
Ca	4524	10747	11151	8593	10438	13072	6969	6251	11856
Ba	2.31	4.22	6.75	6.43	7.47	45.63	32.27	3.64	9.17
Pb	3.20	2.86	5.02	4.50	3.05	3.25	5.13	2.60	3.63
Sr	345	469	361	388	305	388	298	272	426
Zn	0.37	2.29	5.44	10.45	9.88	41.54	35.23	2.34	9.25
Mn	7.86	13.11	13.20	21.63	102.95	18.26	16.67	12.05	16.36
Al	1.88	1.75	1.77	2.00	1.39	1.86	1.79	1.48	2.63
Be	0.012	0.016	0.012	0.014	0.020	0.011	0.011	0.005	0.011
Fe	1.156	0.949	5.18	9.00	4.26	18.67	15.84	5.47	77.34
B	56.95	46.94	31.02	24.01	27.91	19.12	6.41	28.36	45.50
Br	33.40	92.0	41.01	52.17	147.95	154.00	161.75	184.97	165
I	10.28	1.52	4.39	7.50	6.84	11.15	6.33	5.78	6.76

(1)n₁, n₂, n₃ are the numbers of analyses for major components TDS, K + Na, Ca, Mg, SO₄, HCO₃, minor and trace elements Ba, Pb, Sr, Zn, Mn, Al, Be, Fe, B, and elements Br and I, respectively. (2) Br and I are in ×10⁻⁶, the other elements in mg/L. (3) LN, DH and TZ stand for the Lunnan, Donghetang and Central Tarim areas.

comparable with those of waters (up to 2 ~ 6 mg/L Al) from the Tertiary system in the San
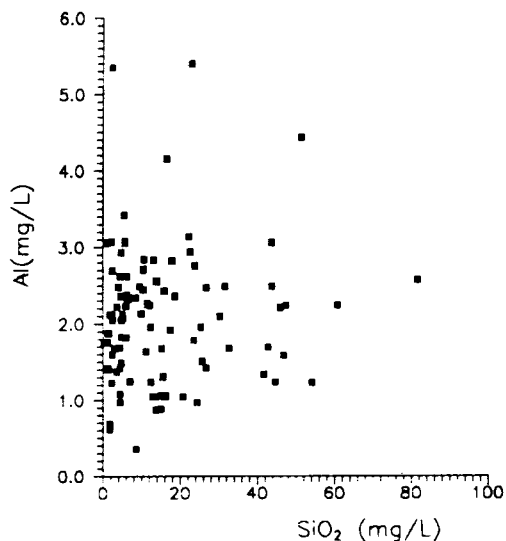
Fig. 3. Scatter diagram showing dissolved Al and SiO_2 concentrations. Up to 3 mg/L to 5.4 mg/L Al can be observed, suggesting the occurrence of organic complexing agents.

Joaquin Basin, and are related to enhanced water-aluminosilicate reactions and high Al stability in waters, suggestive of the occurrence of organic complexing agents (Fisher and Boles, 1990; Cai et al., 1996b, c). Calculations by SOLMINEQ. 88 with the updated database (Giordano and Kharaka, 1994) show that $AlAc^{2+}$ may account for up to 93.89 mole% of the total Al, but normally less than 30 mole% (Table 2). The dissolved SiO_2 concentrations are in the range of 0.2 - 81.8 mg/L, mostly from 10 mg/L to 40 mg/L, and a little lower than those in the Frio Formation (Oligocene) from Texas Gulf Coast (Mortan and Land, 1987), and in Tertiary from the San Joaquin Basin. Although Si-organic complexes have been found (Bennett and Siegel, 1987), they do not occur in waters from the Tarim Basin as viewed from calculations using SOLMINEQ. 88 with the present thermodymanics database.

Table 2. Major Al occurrence and percentage of the total Al

Well No	Formation	Analytical result (mmol/L)		Modeling result (%)				pH
		Acetate	Al	$AlAc^{2+}$	$Al(OH)^{2+}$	$Al(OH)^{2+}$	$Al(OH)^{4-}$	
DH11	C_{III}	26.23	0.094	93.89	6.09	0.028	0.00084	3.84
J102	T	2.98	0.10	0.01	11.54	0.0026	88.48	6.21
LN15	O	1.60	0.090	1.80	93.19	0.071	4.91	5.13
LN56	C_{III}	1.48	0.052	0.016	33.08	0.0026	66.88	5.83
LN3	T_{III}	1.66	0.094	0.32	77.70	0.030	21.96	5.48
LN56	C_I	3.13	0.084	1.63	80.94	0.069	17.36	5.41
T101	N_{1j}	1.04	0.093	tr	0.0011	tr	100.00	8.24
DH2	C	4.85	0.27	39.98	59.84	0.10	0.081	4.32
TZ401	C_I	0.62	0.040	33.16	63.11	3.02	0.31	5.95

Other elements

Analysis of oilfield waters shows that Li concentrations mainly range from 2.0mg/L to 10.0mg/L and Sr from 200mg/L to 450mg/L. In view of the average values of different systems, there occur Fe- and B-enriched waters in the Cambrian and Ordovician strata; in the Carboniferous strata, Fe and B are relatively depleted in Central Tarim, Ba and Zn are abundant in the Lunnan and Donghetang areas; Mn is enriched in the Triassic strata; B is enriched, and Fe and Mn are depleted in the Tertiary strata. Relatively Be-enriched waters occur in the Mesozoic and Cenozoic, and Be is absent in the Paleozoic. A positive correlation exists between B concentrations and TDS in the Tertiary, Jurassic and Triassic systems, but not in the Paleozoic (Table 1). An increase in Li concentrations during deeper burial can be found in the profile of oil-bearing layers of Well LN3 (Fig. 4), TZ4, DH2 and YM901. And all the data for 55 water sam-
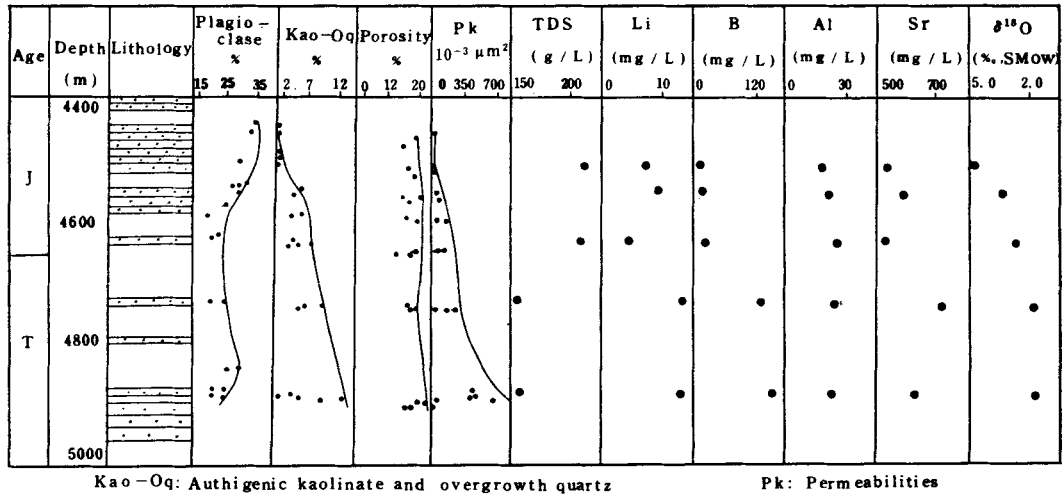
Age	Depth (m)	Lithology	Plagio-clase % 15 25 35	Kao-Oq % 2 7 12	Porosity % 0 12 20	Pk 10⁻³ μm² 0 350 700	TDS (g/L) 150 200	Li (mg/L) 0 10	B (mg/L) 0 120	Al (mg/L) 0 30	Sr (mg/L) 500 700	δ¹⁸O (‰ SMOW) 5.0 2.0
J	4400 4600											
T	4800 5000											

Kao-Oq: Authigenic kaolinate and overgrowth quartz   Pk: Permeabilities

Fig. 4. Diagram showing covariation among mineral contents, reservoir porosity and water chemistry, suggesting enhanced water-rock interaction and secondary porosity and permeability.
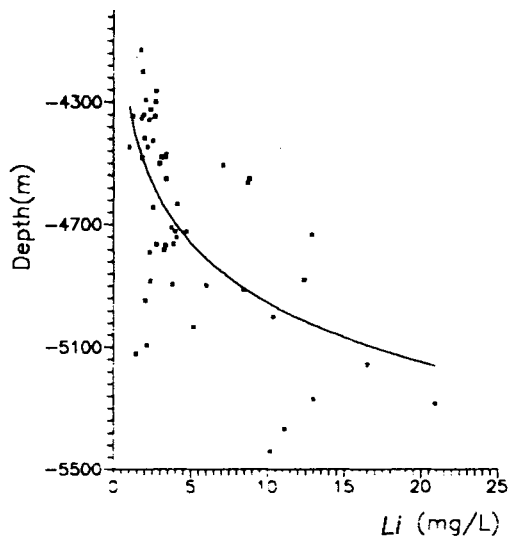

Fig. 5. Scatter diagram showing log-function relationship between Li and depth in the Lunnan area.

ples from the Lunnan area with a similar sedimentary and burial history show the existence of a functional relationship between Li concentrations and depth (Fig. 5). So, the relationship between Mg and Li can be used to calculate the paleotemperatures of reservoirs (Kharaka and Mariner, 1989; Land and Macpherson, 1992). From Fig. 4, an increase in Li and B concentrations and a positive shift of $\delta^{18}O$ are in concert with a decrease in detrital plagioclase and an increase in authigenic kaolinate and quartz overgrowth, suggesting enhanced dissolution of plagioclase and reprecipitation of dissolved species at higher temperature. And this is supported by more than 600mg/L Sr in oilfield waters from clastic reservoirs, much higher than the average value of individual systems. The increase of Li, B and Sr and the positive shift of $\delta^{18}O$ are also considered to have resulted from dissolution of crustal detrital minerals, i. e., enhanced water-rock interaction in Gulf Coast sandstones (Land and Macpherson, 1992).

Analysis of 70 oilfield water samples shows that Br has a wide range among oilfield waters of different ages (Table 1). Less than 95×10^{-6} Br occurs in the Mesozoic (except Triassic) and Cenozoic strata, approximately 150×10^{-6} in the Triassic system, and more than 150×10^{-6} in the Paleozoic on average. Very low Br, only from 21×10^{-6} to 26×10^{-6}, but high I concentrations ranging from 12.9×10^{-6} to 14.4×10^{-6}, occur in the Upper Tertiay series in
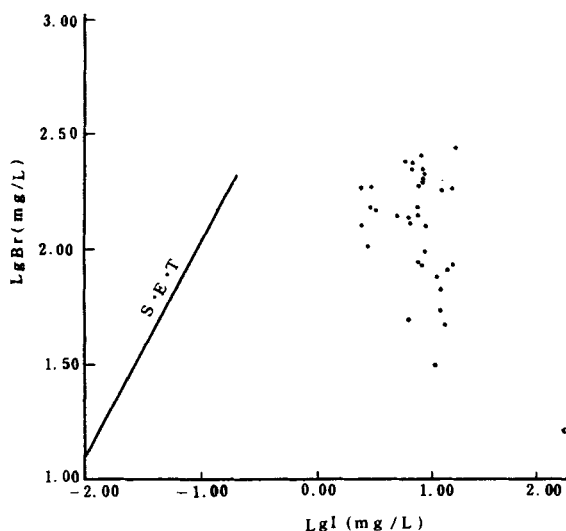
Fig. 6. Scatter diagram showing relationship between Br and I. Seawater Evaporation Trajectory (S. E. T.) is also shown for reference. There is no or negative covariation between Br and I, suggesting different sources of Br and I.

the Kekeya oilfield in front of the Kunlun Mountains. About 50% of the oilfield waters in Cambrian and Ordovician reservoirs contain 150×10^{-6} to 200×10^{-6} Br, even up to 250×10^{-6} to 300×10^{-6}. Relatively high Br in the Triassic system is related to upward migration of waters and hydrocarbons from the Cambrian and Ordovician systems, and their mixing. So, it can be concluded that relatively low Br concentrations occur in terrestrial formation water, and high Br in marine environment. Br increases at deeper burial or higher temperature, suggesting that Br is controlled by the sedimentary enviroment and evapo-concentration. Abundance of I relative to Br in oilfield waters is shown by the relationship between Br and I (Fig. 6), and is considered to be sourced from degradation of organic matter (Collins, 1975; Fisher and Boles, 1990). Although both Br and I are brine elements, a negative correlation or no obvious correlation between Br and I suggests that they are of different origins. Also, it is impossible for organic matter to be degradated to produce enough Br (Ritterhouse, 1967). So, the chemical evolution of oilfield waters can be shown by the correlation with the evaporation curve of seawater established by Carpenter (1978) (Connolly et al, 1990a; Wilson and Long, 1993a, b; Egeberg and Aagaard, 1989).

Relations between brines and evaporated seawater

Fig. 7 shows the relationship between brines of oilfield waters from the Tarim Basin and evaporated seawater. The CF (CF = Ca + Mg + Sr-SO_4-HCO_3, in meq/L) relative to Br is considered to remain unchanged during the specified reactions as sea water is evaporated (Carpenter, 1978; Connolly et al., 1990a), so it can be used to account for the whole effect of water-rock interaction. All these waters are characterized by relative absence of Mg, abundance of Cl, Ca, Sr and CF (Fig. 9).

Except waters from Well TZ4, all plot above Seawater Evaporation Trajectory (S. E. T) on log Cl-log Br diagram, suggesting Cl enrichment. Cl-enriched waters may be generated by halite dissolution and fluid flow. In the Tarim Basin, gypsum and salt beds occur in the Carboniferous section, salt domes are drilled in Xiang No. 1 Well, gypsum and salt-bearing beds in Mancan No. 1 Well, where high TDS and Cl- enriched waters are located, suggestive of the occurrence of halite dissolution. Dissolved chloride can be advected and dispersed up to 3 km (Hanor, 1994), a more than 100m (Bjφrlykke and Gran, 1994) distance from salt domes. Waters from Well TZ4 are characterized by Cl depletion and low TDS, but impossible to have resulted from halite recrystallization (e. g. Connolly et al, 1900a), and suspected to be due to freshwater mixing. Regional data show that low TDS, high hydrolaulic potential occur in the northwestern part where meteoric water was recharged (Cai et al., in prep.). Meteoric water
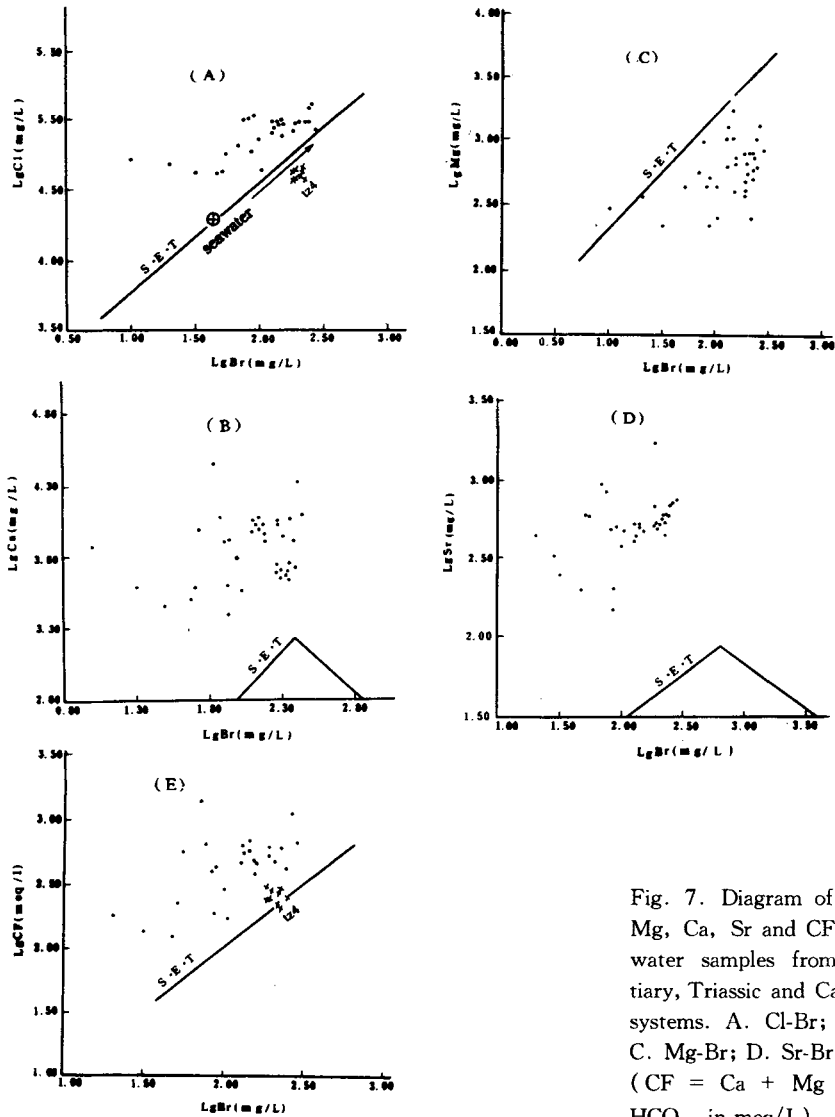
Fig. 7. Diagram of Br vs Cl, Mg, Ca, Sr and CF for oilfield water samples from the Tertiary, Triassic and Carboniferous systems. A. Cl-Br; B. Ca-Br; C. Mg-Br; D. Sr-Br; E. CF-Br ($CF = Ca + Mg + Sr-SO_4-HCO_3$, in meq/L).

moves along the C/S or C/O unconformity, and flushes and mixes with connate waters in the TZ4 structure. Waters are characterized by Ca-enrichment and Mg-depletion, corresponding to the major cation ternary diagram, suggesting dissolution of feldspar and dolomization of calcite. Gypsum and laumontite dissolution in Tertiary sandstones is an important source of Ca.

Alkalinity and organic acid anions (OAA)

   Occurrence and distribution of OAA   Organic acid anions analyzed in oilfield waters from the Tarim Basin include formate, acetate, propionate, and butanoic acid, following the order of acetate > > formate > propionate > butanoic acid with respect to their abundances. OAA range from 2 – 4094 mg/L, mostly less than 1500mg/L over a temperature range of 81 –

142℃, and acetate accounts for 40% − 80% of the total OAA. Absence of acetate dominance at the temperature less than 95℃ can result from methanogenic bacteria activity with acetate preferentially degraded relative to other types of organic acids. Difunctional organic acids have not been detected in all oilfield waters, whereas high organic acid anions occur over the temperature range from 95 − 140℃ (Fig. 8), corresponding to burial depths from 4300 m to 6000 m. Peak values of organic acid anions occur from 4300 m to 4800 m , i. e., 106 − 118℃, in the Triassic and Jurassic systems in the Lunnan area, and from 5400 m to 5900 m, i. e., 130 − 139℃, in the Carboniferous reservoir strata in the Donghetang area. The temperature range in which OAA are abundant in the Tarim Basin is slightly different from 80 − 120℃ interval (Surdam et
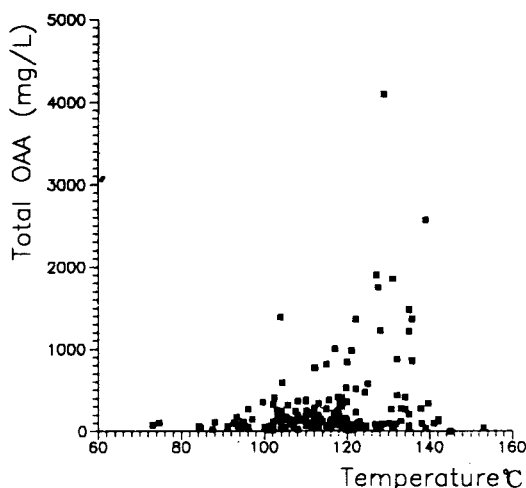

Fig. 8. Organic acids and anions concentrations as a function of temperature.

al., 1989; MacGowen et al., 1987), but is within the range between 80 − 200℃ (Carother and Kharaka, 1978), and this argues against OAA thermal instability at about 120℃, which is supported by Shock (1988), Helgeson et al. (1993) and so on. From OAA concentrations reported in the literature, the decreasing sampled waters above ~ 125℃ may result from decreased hyperthermobarophilic microbial activity and/or fewer oil-bearing intervals at higher temperatures (Helgeson et al., 1993). Data from the Tarim Basin where the oil reservoir temperatures are mainly higher than 125℃ in the Carboniferous system (except TZ area) and below show that high OAA may occur at high temperatures. In the Tertiary and Cretaceous systems, relatively low OAA concentrations with a low maxmium value of 188 mg/L are observed. From the Jurassic to Cambrian system, the highest OAA concentration of individual system is more than 1200 mg/L (Table 3), which is consistent with the distribution of main oil and gas generating layers. It can also

Table 3. Distribution of the highest concentrations of OAA in different systems

System	Analysis No.	Peak value (mg/L)
K	13	188
J	19	4094
T	53	1391
C	33	1900
S	2	1754
O	19	2571
∈	2	1217

be found that there exist high contents of OAA in oilfield waters near the unconfomities. Among the 185 water samples, 10 are produced from reservoirs about 50 m away from the unconformities. The OAA concentrations of 6 (i. e., 60%) samples are more than 800 mg/L, and of all the water samples (>800 mg/L), 33% occurs near the unconformities. For example, nearby the J/C unconformity of DH2, OAA concentrations come up to 873 mg/L with less than 280 mg/L in the upper and lower waters. It can be concluded that abnormally high OAA occur nearby the unconformities.

Source of OAA   OAA in oilfield waters are generally considered to be generated from maturation of kerogens in mudstones, which may be the main source of OAA during progressive burial of sandstone/shale and carbonate systems in the Jurassic—Triassic and Cambrian—Ordovician systems in the Tarim Basin. Although microbes are considered to be depleted in OAA, especially acetate, at low temperatures (Carother and Kharaka, 1978; Means and Hubbard, 1987), biodegradation of hydrocarbons can also produce OAA (Jobson et al., 1979; Machel et al., 1995; Shock, 1988; Helgeson et al., 1993; Kharaka et al., 1993; Cai et al., 1996a). However, it is of great debate on whether these bacteria are aerobic or anaerobic. And it cannot be ruled out that the above product is due to the activity of different types of bacteria. In the Tarim Basin, high OAA values near the unconformities are suggested to be the result of biodegradation of crude oils (Cai chunfang et al., 1996b), as is supported by high Pr/nC_{17}, Ph/nC_{18} ratios and unresolved complex compounds ("UCMs") of extract oils from bitumen-bearing sandtones in gas chromatographs. And low δD and TDS, high $(K + Na)/TDS$, HCO_3/TA and $\gamma Na/\gamma Cl$ of oil field waters adjacent to the unconformity indicate an in flux of meteoric waters which carried aerobic bacteria and oxidants, and caused oxidation or biodegradation of oils. And it is the main reason for the occurrence of high OAA concentrations there. OAA can be sourced from redox reactions between mineral oxidants and hydrocarbons (Surdam et al., 1993), or thermochemical sulfate reduction (Machel, 1987; Machel et al., 1995; Cai Chunfang et al., 1997), which may supply more oxygen than simple thermal alteration of crude oils (Kharaka et al., 1993), and more OAA are expected to be generated. Up to 1217 mg/L and 2571 mg/L of OAA occur in the depth interval of 5956 – 6125 m in Well TZ1, and 5981 – 6160 m in Well LN13, respectively, with reservoir temperature ranging from 135℃ to 140℃ . Occurrence of gypsum pseudocrystals, up to 2.56% sulfides in carbonate rock and 780 mg/L dissolved H_2S and so on indicate that SO_4 in oilfield waters and gypsum are reduced into sulfides. Black solid bitumen is found in intercrystal dissolution porosity and fluid inclusions, and its homogenization temperatures range mainly from 100 – 130℃ , up to 150 – 180℃ , which are near or above the lower limit from 100 to 140℃ (Machel et al., 1995), indicating that OAA are generated by TSR of crude oils.

Influence of OAA on alkalinity   Oilfield waters are typically low in acidity with pH ranging mostly from 5.5 to 6.5 measured on the surface. But measured pH values are affected both by degassing of CO_2 and H_2S due to pressure release and by oxidation of Fe. So, the measured pH values may be much different from those under reservoir conditions with a deviation up to 2.5 unit (Willey et al., 1975; Kharaka et al., 1986). Thus, the total alkalinity $(HCO_3^- + CO_3^{2-} + HS^- + OAA)$ is adopted. OAA concentrations may contribute mostly 30% to 70% to the total alkalinity among 114 water samples, the percentage of waters with OAA contribution more than 70%, up to 92%, is 21.1%, indicating that OAA control the fluid alkalinity.

Influence of OAA on secondary porosity   High contributions of OAA and complexing agents of Al are related to the formation of secondary porosity. There exists a good correlation between high OAA and good reservoir property. For example, high OAA occur in the LN3 – LN31 and LN10 regions in the Lunnan oilfield, adjacent to LN58 and LN53 in the Jilake oilfield in T_{II} unit of the Triassic system. Reservoir of T_{II} unit from Well LN58 with more than 1300 mg/L OAA has a porosity range mainly from 17% to 25% and a permeability from 300 md to 1000 md. Waters from oil-bearing reservoirs at the 5845 – 5870 m depth interval at the "DH sandstone" Group of the Carboniferous system in the DH11 section contain up to 1371 mg/L OAA, corresponding to a sandstone porosity from 12% to 17% and a permeability from

10 md to 237 md. The case occurs also in the upper part from 50 m to 120 m of "DH sandstone" Group with a porosity mainly from 13% to 18% and a permeability from $20 \times 10^{-3} \mu m^2$ to $100 \times 10^{-3} \mu m^2$, whereas poor porosity occurs in the water-saturated intervals with the porosity from 10% to 14% and the permeability from 5 md to 10 md. And the case is true for North Cole Levee (Boles, 1991), positive correlations among OAA concentrations, Al and Si, and high reservoir porosity in oil-bearing depth intervals suggest enhanced mineral dissolution and secondary porosity.

Calculation of mineral dissolution-precipitation trends

Mineral dissolution-precipitation tends can be evaluated by comparing the ion activity product (AP) of the minerals to their equilibrium constants (K_T) at a specific temperature and pressure. And the evaluation is carried out using the geochemical computer code SOLMINEQ. 88 with Pitzer formulation and updated thermodynamic database recently reported by Giordano and Kharaka (1994). The program is run at calcite, occasionally dolomite, saturation to specific
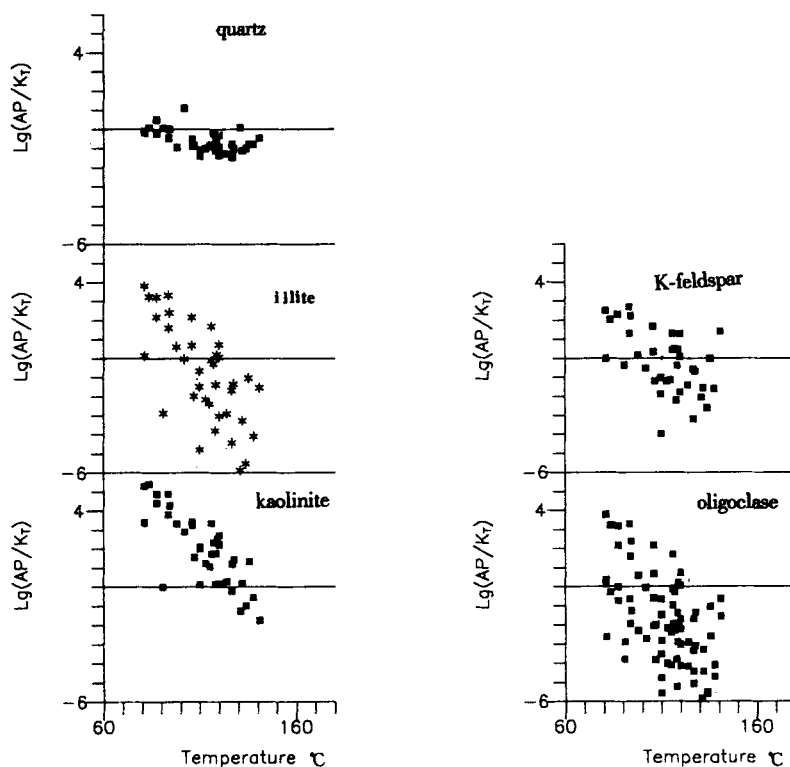

Fig. 9. Scatter diagrams showing mineral stability vs. temperature.

temperature and pressure to recalculate the pH values of waters suggested by Connolley et al. (1990), and acetate is used as OAA. The modeling results of 43 oilfield water samples from the Triassic and Jurassic systems in the Lunnan area, and from the Carboniferous in Donghetang and Central Tarim show that oligoclase is unsaturated and tends to dissolve at 81°C to 132°C; kaolinite is oversaturated and tends to be precipitated at temperatures lower than 132°C, and is unstable at more than 132°C; quartz is close to equilibrium and that K-feldspar is stable between 81°C and 105°C, and is variable in stability at more than 105°C (Fig. 9). From

the above, it can be concluded that oligoclase is of higher solubility than K-fledspar while medi-ated by OAA, and that plagioclase dissolution and kaolinite precipitation are the main diagenetic factors controlling secondary porosity. And it is consistent with petrographic observations (Zhu et al., 1990; Cai, et al., 1995; Zhai et al., 1995).

Hydrogen, oxygen stable isotopes

Oxygen and hydrogen isotopic analyses for 73 water samples show that δD values range from $-72.50‰$ to $-26.80‰$ (SMOW) and $\delta^{18}O$ from $-11.50‰$ to $4.99‰$ (SMOW). Those waters are meteoric or diluted with drilling fluids, which are distributed near the Global Meteroric Water Line (MWL) with equation $\delta D = 8 \times \delta^{18}O + 10$ (Craig, 1961), including waters from the Kongque River, the Jurassic section of Well LN61 and the Lower Tertiary of Well LN21 and LN61.

The waters from Cenozoic and Mesozoic terrestrial sedimentary environments can be subdi-vided into three groups (Fig. 10a) :

Waters of Group I are evaporated connate meteoric waters, and those of Group II are mainly controlled by diagenetic modification, some of which are mixed with later meteoric wa-ters. The former is characterized by $\delta^{18}O$ values varying between $-1.05‰$ and $+3.87‰$ (SMOW) and δD from $-60.30‰$ to $-32.60‰$(SMOW). Group II has lighter δD and $\delta^{18}O$ than Group I , with δD values ranging from $-64.30‰$ to $-43.90‰$ (SMOW) and $\delta^{18}O$ from $-5.31‰$ to $+2.72.‰$ (SMOW). Group I occurs in the sedimentary environment of dry salt lake and red river in the Cretaceous, Tertiary, and in the strata containing gypsum and salt beds. From Fig. 10A it is seen that all waters of Group I plot towards the MWL, and a least squares fit to all the data intersects the meteroric water line at $\delta D = -55.91‰$ (SMOW) and $\delta^{18}O = -8.24‰$ (SMOW), suggesting that Group I is evolved from meteoric waters. Meteoric water evaporation at low humidity can also produce a heavier isotopic composition (Knauth and Beeunas, 1986). Waters of Group II are produced from the Jurassic and Triassic reservoirs, where the strata contain thin coal beds and carbonaceous mudstone, in-dicative of humid climate at the time of deposition. And the strata are considered to be continuous lake sediments. So, evaporation is not a main factor leading to oxygen isotope evolution. Linear relationship exists among all waters from Group II with intersection to MWL at $\delta D = -63.68‰$, $\delta^{18}O = -9.21‰$ (SMOW), close to those from nowaday Kongque River ($\delta D = -72.50‰$, $\delta^{18}O = -11.5‰$ (SMOW)). Positive shift in $\delta^{18}O$ may be related to oxygen stable isotope exchange between oilfield water and alumino-silicate minerals and calcite, dolomite, and enhanced water-rock interaction (Fisher and Boles, 1990; Land and Macpher-son, 1992), which is supported by OAA occurrence, and petrographic observations such as ex-tensive dissolution and transformation of plagioclase to kaolinate and quartz, recrystallization of calcite and dolomite at relatively high temperatures (Zhu et al., 1990; Cai Chunfag et al., 1995). Water-rock interaction is considered to be a main factor controlling oxygen isotope shift in the Jurassic and Triassic reservoirs. Positive δD shift may result from evaporation of meteoric water and gypsum dehydration (Knauth and Beeunas, 1986), but gypsum does not occur in the strata. Consequently, meteoric water evaporating may be a main reason for heavier δD val-ues under humid climate conditions. In Group II , those oilfield waters with very negative $\delta^{18}O$ and δD values, which lie at the left of the best fit line, may be the mixture of meteoric water and evaporated or diagenetically modified connate (meteoric) water from the J/C and T/C un-conformities. Freshwater is considered to permeate along the unconformities in the Late Yen-shanian to the Early Himalaya Orogeny, and then mixing took place. For example, oilfield wa-

ters with light δD values and variable $\delta^{18}O$ are found at greater burial depth than 5450 m of the Jurrassic section of Well DH2 near the J/C unconformities (5558.5 m), at the bottom of the Triassic of Well LN18 and LN57. But, it seems to be reasonable that very negative δD values result from deuterium exchange between water and hydrocarbon (Fisher and Boles, 1990).

Marine Paleozoic oilfield waters include Carboniferous and Cambrian-Ordovician oilfield waters.

Carboniferous oilfield waters are the mixture of meteoric water and evaporated seawater as is shown in Fig. 10B. All the data slope to MWL with the intersection at $\delta D = -70.96‰$ and $\delta^{18}O = -10.12‰$ (SMOW). This kind of isotopic composition distribution pattern is suggested to be the remanant of evapo-concentrated seawater, which is infiltrated by later meteoric water (Connolly and Walter, 1990b; Wilson and Long, 1993a). And the explanation is in concert with low Cl/Br ratios and the occurrence of salt beds.
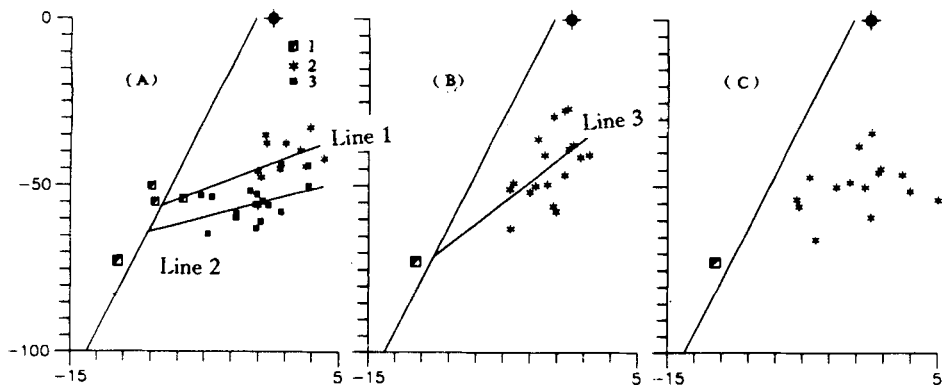

Fig. 10. Relationship between hydrogen and oxygen isotope compositions for the R-K and J-T (A), C (B) and ∈-O (C) systems. Lines 1, 2 and 3 are representative of the best fit of data from R-K, T-J, C, respectively. A. terrestrial Cenozoic and Mesozoic; B. marine Carboniferous; C. Cambrian and Ordovician. 1. Kongque River or diluted by drilling waters; 2. Tertiary and Cretaceous, Group I; 3. Jurassic and Triassic, Group II.

Cambrian-Ordovician oilfield waters are characterized by small variations in δD from $-65.60‰$ to $-33.90‰$ (SMOW) relative to $\delta^{18}O$ from $-5.45‰$ to $4.99‰$ (SMOW) (Fig. 10C), suggesting that they are mainly controlled by water-rock interaction. Although this explanation is difficult to account for lower $\delta^{18}O$ values than the present SMOW, Ordovician seawater is ca. $5.5‰$ lighter in $\delta^{18}O$ than SMOW suggested by Brand and Veizer (1980), indicating that all the oilfield waters are heavier than seawater in that period. Morever, the data neither show any linear relationship nor slope and intersect to the MWL. From the above, it implies that meteoric water mixing is not a main factor affecting isotopic evolution. Waters characterized by the isotopic compositions of $\delta D = -53.8‰$ and $\delta^{18}O = 4.99‰$ (SMOW) in the Ordovician of Well LN3, and $\delta D = -51.3‰$ and $\delta^{18}O = 2.92‰$ (SMOW) in the depth interval of $6450 - 6503.3$ m in the Cambrian system can not simply be considered to be a product of mixing and subsequently oxygen isotope exchange with oxygen-bearing minerals (Kharaka et al., 1973) because the Cambrian system has not been found to be uplifted to the surface and infiltrated. But, mudstone and limestone in the Cambrian-Ordovician systems are considered to be main source rocks, and when interlayer water is released, hydrocarbons are generated and expelled during diagenesis, hydrocarbons and waters migrating to the reservoirs may exchange

D and O isotope with connate waters, resulting in a decrease in δD. However, waters from clay minerals also cause a decrease in $\delta^{18}O$. Consequently, hydrocarbon-water interactions are required to explain the occurrence of heavy $\delta^{18}O$, which causes no change in $\delta^{18}O$ (Fisher and Boles, 1990). After emplacement of crude oils into reservoirs, thermochemical sulfate reduction can result in the generation of H_2S gas and some organic acids and anions, which thus enhance water-rock interaction and positive $\delta^{18}O$ shift.

References

Bennett, P. and D. I. Siegel, 1987, Increased solubility of quartz in water due to complexing by organic compounds: Nature, v. 326, p. 684 – 686.

Barth, T. and K. Bjфrlykke, 1993, Organic acids from source rock maturation: generation potentials, transport mechanisms and relevance for mineral diagenesis: Applied Geochemistry, v. 8, p. 325 – 337.

Bjфrlykke, K. and K. Gran, 1994, Salinity variations in North Sea formation waters: implications for large-scale fluid movements: Marine and Petroleum Geology, v. 11, n. 1, p. 5 – 9.

Boles, J. R., 1991, Plagioclase dissolution related to oil residence time, North Coles Levee field, California: AAPG. Bul., v. 75, p. 544.

Cai Chunfang, Mei Bowen, Ma Ting, Chen Chuanping, and Liu Changqing, 1996a, Hydrocarbon-water-rock interactions in the diagenetically altered system nearby unconformities of Tarim Basin: Chinese Science Bull., v. 41, n. 19, p. 1631 – 1635.

Cai Chunfang, Mei Bowen, Zeng Fangang, Fang Xiaolin, and Ma Ting, 1996b, Water-rock interaction in Tarin basin: constraints from oilfield geochemistry, in Abstracts of 30th International Geological Congress: Beijing, v. 3, p. 31.

Cai Chunfang, Mei Bowen, Ma Ting, Zhao Hongjing, and Fang Xiaolin, 1997, The source, distribution of organic acids and anions in oil field water and their effects on diagenesis in Tarim Basin: Acta Sedimentolodica Sinica, v. 15, n. 3 (in Chinese, in press).

Cai Chunfang, Mei Bowen, Ma Ting, and Liu Changqing, 1995, Diagenetic reactions in Jurrassic-Triassic system of North Tarim: Petroleum and Natural Gas Geology, v. 16, p. 259 – 264 (in Chinese).

Cai Chunfang, Mei Bowen, and Li Wei, 1996c, Oilfield hydrogeochemistry of Tarim Basin: Geochimica, n. 6, p. 614 – 623.

Collins, A. G., 1975, Geochemistry of oilfield waters: Elsevier, Amsterdam, 496p.

Connolly, C. A., L. M. Walter, H. Baadsgaard, and F. J. Longstaffe, 1990a, Origin and evolution of formation waters, Alberta Basin, Western Canada Sedimentary Basin. I. Geochemistry of formation waters: Applied Geochemistry, v. 5, p. 375 – 395.

Connolly, C. A., L. M. Walter, H. Baadsgaard, and F. J. Longstaffe, 1990b, Origin and evolution of formation waters, Alberta Basin, Western Canada Sedimentary Basin. II. Isotope systematics and water mixing: Applied Geochemistry, v. 5, p. 397 – 413.

Craig, H., 1961, Isotopic variations in meteoric waters: Science, v. 133, p. 1702 – 1703.

Egeberg, P. K. and P. Aagaard, 1989, Origin and evolution of formation waters from oilfields on the Norwegian shelf: Applied Geochemistry, v. 4, p. 131 – 142.

Fisher, J. B. and J. R. Boles, 1990, Water – rock interaction in Tertiary sandstones, San Joaquin basin, California, U. S. A.: Diagenetic controls on water composition: Chemical Geology, v. 82, p. 83 – 101.

Giordano, T. H. and Y. K. Kharaka, 1994, Organic ligand distribution and speciation in sedimentary basin brines, diagenetic fluids and related ore solutions, in Parnell, ed., Geofluids: origin, migration and evolution of fluids in sedimentary basins: Geological Society Special Publication, v. 78, p. 175 – 202.

Hanor, J. S., 1994, Physical and chemical controls on the composition of waters in sedimentary basins: Marine and Petroleum Geology, v. 11, p. 31 – 45.

Helgeson, H. C., A. M. Knox, C. E. Owens, and E. L. Shock, 1993, Petroleum, oilfield waters, and authigenic mineral assemblages: Are they in metastable equilibrium in hydrocarbon reservoirs? Geochimica et Cosmochimica Acta, v. 57, p. 3295 – 3339.

Jobson, A. M., F. D. Cook, and D. W. S. Westlake, 1979, Interaction of aerobic and anaerobic bacteria in petroleum biodegradation: Chemical Geology, v. 24, p. 355 – 365.

Kharaka, Y. K., R. W. Hull, and W. W. Carother, 1985, Water-rock interactions in sedimentary basins, in D. C. Gautier et al, eds., Relationship of Organic Matter and Mineral Diagenesis: Soc. Econ. Geol. Paleont., Short Course, n. 17, p. 79 – 272.

Kharaka, Y. K., L. M. Land, and W. W. Carothers, 1986, Role of organic species dissolved in formation waters from sedimentary basins in mineral diagenesis, in Gautier, D. L., ed., Roles of organic matter in sedimentary diagenesis: SEPM Special Publications, v. 38, p. 111 – 122.

Kharaka, Y. K., W. D. Gunter, P. K. Aggarwal, E. H. Perkins, and J. D. DeBraal, 1988, SOLMINEQ. 88: A computer program for geochemical modeling of water-rock interactions: USGS Water Resources Invest, Report 88 – 4227, Menlo Park, CA., 420p.

Kharaka, Y. K., P. D. Lundegard, G. Ambats, W. C. Evans, and J. L. Bischoff, 1993, Generation of aliphatic acid anions and carbon dioxide by hydrous pyrolysis of crude oils: Applied Geochemistry, v. 8, p. 317 – 324.

Kharaka, Y. K., F. A. Berry, and I. Friedman, 1973, Isotopic composition of oil-field brines from Kettleman North Dome, California, and their geologic implications: Geochim. Cosmochim. Acta, v. 37, p. 1899 – 1903.

Knauth, L. P. and M. A. Beeunas, 1986, Isotope geochemistry of fluid inclusions in Permian halite with implications for the isotopic history of ocean water and origin of saline formation waters: Geochimica et Cosmochimica Acta, v. 50, p. 419 – 433.

Land, L. S. and G. L. Macpherson, 1992, Origin of saline formation waters, Cenozoic section, Gulf of Mexico sedimentary basin: AAPG Bull, v. 76, p. 1344 – 1362.

Machel, H. G., H. R. Krouse, and R. Sassen, 1995, Products and distinguishing criteria of bacterial and thermochemical sulfate reduction: Applied Geochemistry, p. 373 – 389.

Means, J. L. and N. J. Hubbard, 1987, Short-chain aliphatic acid anions in deep subsurface brines: A review of their origin, occurrence properties and importance and new data on their distribution and geochemical implications in the Palo Duro Basin, Texas: Org. Geoch., v. 11, p. 177 – 191.

Ritterhouse, G., 1967, Bromine in oilfield waters and its use in determining possibilities of origin of these waters: AAPG, Bull, v. 51, p. 2430 – 2440.

Shock, E. L., 1988, Organic acid metastability in sedimentary basins. Geology, v. 16, p. 886 – 890.

Surdam, R. C., L. J. Crossey, E. S. Hagen, and H. P. Heasler, 1989, Organic-inorganic interaction and sandstone diagenesis: AAPG Bull., v. 73, 23p.

Surdam, R. C., L. J. Crossey, and D. B. MacGowan, 1993, Redox reactions involving hydrocarbons and mineral oxidants: A mechanism for significant porosity enhancement in sandstones: AAPG Bull., v. 77, n. 9, p. 1509 – 1518.

Tong Xiaoguang and Liang Digang, 1992, Collection of Petroleum and gas exploration in Tarim basin: Urumqi, Xinjiang Hygiene Press of Science and Technology, p. 411 – 456 (in Chinese).

White, D. E., 1965, Saline waters of sedimentary rocks, in A. Young and J. E. Galley, eds., Fluids in subsurface environments: AAPG Mem., v. 4, p. 342 – 366.

Wilson, T. P. and D. T. Long, 1993a, Geochemistry and isotope chemistry of Michigan Basin brines: Devonian formations: Applied Geochemistry, v. 8, p. 81 – 100.

Wilson, T. P. and D. T. Long, 1993b, Geochemistry and isotope chemistry of Ca-Na-Cl brines in Silurian strata, Michigan Basin, U. S. A.: Applied Geochemistry, v. 8, p. 507 – 522.

Willey, L. M., Y. K. Kharaka, T. S. Presser, J. B. Rapp, and I. Barnes, 1975, Short chain aliphatic acid anions in oilfield waters and their contribution to the measured alkalinity: Geochimica et Cosmochimica Acta, v. 39, p. 1707 – 1711.

Zhai Yonghong, Liu Hengguo, Guo Jianghua, Xiao Chuantao, and Luo Chuanrong, 1993, Diagenesis and pore evolution of Carboniferous clastic rocks in Central Tarim: Petroleum and Natural Gas Geology, v. 16, p. 254 – 258 (in Chinese).

Zhu Guohua, Wang Haoyi, Yao Genshun, 1993, Pore types and origin of high porosity at deep burial, in Qiu, Y. et al., eds., Collection of Chinese Petroleum-bearing Reservoir Study (Continued): Beijing, Petroleum Industry Publishing House, p. 240 – 261 (in Chinese).